



Journal reviewer's marked copy.

Reviewer's margin comments refer to yellow-highlighted text.

Blue highlighting was for the reviewer's comprehension, and may be ignored.

# 1 A Theory of Earthquake Prediction

2

3 Jeen-Hwa Wang

4 Institute of Earth Sciences, Academia Sinica, Taipei, Taiwan, ROC

5 E-mail: jhwang@earth.sinica.edu.tw

6

7

8

## 9 Abstract

10 In this study, the pre-seismic strain of an earthquake is considered as a fundamental  
11 and important precursor. Based on the Voight's equation for material failure, we  
12 theoretically investigate the physical basis on predicting the failure time, magnitude,  
13 and location of a forthcoming earthquake in terms of pre-seismic strains generated on  
14 or near the related fault where the event will happen. The  $\log(T)$ - $M$  relationship is  
15 built up. Results exhibit that the failure time depends on the strain rate and two  
16 parameters of the Voight's equation; while the magnitude is associated with the  
17 precursor time, two parameters of the Voight's equation, and the exponent of the  
18 scaling law between the strain and the fault length. The location of the forthcoming  
19 earthquake may be qualitatively estimated from the localities of observation sites  
20 where the pre-seismic strains are observed. In addition, the anomalous geoelectric and  
21 geochemical signals prior to earthquakes are also taken into account as precursors.  
22 Their  $\log(T)$ - $M$  relationships are derived. The precursor times of geoelectric signals  
23 and those of the geochemical signals are, respectively, the same and shorter than that  
24 of the pre-seismic strains.

The abstract must stand alone. It is incomprehensible unless variables  $T$  and  $M$  are defined.

Precursory strain?

25

26 **Keywords:** Earthquake prediction, strain, failure time, magnitude, location,  
27 Voight's equation, fault length

28



## 29 1 Introduction

30

31 The ruptures of earthquakes, especially for large ones, are usually preceded by  
32 complex physical and chemical processes which may produce the so-called precursors  
33 (e.g., Atkinson, 1984; Main and Meredith, 1989; Main, 1999; Zaccagnino and  
34 Doglioni, 2022). Hence, a significant way to reduce seismic hazards is the prediction  
35 of forthcoming earthquakes based on observations of reliable precursors. Since Milne  
36 (1880) first addressed this viewpoint in the nineteenth century, earthquake prediction  
37 has been a challenging problem for earthquake scientists (e.g., Knopoff, 1996). Aki  
38 (1989, 2009) assumed that earthquakes are predictable and earthquake scientists  
39 should inform the probability of the occurrence of an earthquake with a specified  
40 magnitude, place, and time window to the government and the public for mitigating  
41 hazards. Although the earthquake prediction seems successful for few large events,  
42 including the 1975 Haicheng, China, earthquake (cf. Wang et al., 2006), it has been  
43 long a debatable problem of earthquake science. Numerous earthquake scientists  
44 address that earthquakes can be predicted, but some others stand for the opposite  
45 viewpoint (e.g. Geller, 1997; Geller et al., 1997). The latter were mainly based on the  
46 reasons that the brittle crust is quite disordered and complicated (cf. Savage et al.,  
47 2010) and it sometimes exists in the critical state (cf. Bak, 1996). The two conditions  
48 will reduce the predictability of forthcoming earthquakes. However, disorder and  
49 complexity within a single fault could be much lower than those in the brittle crust or  
50 a fault system. A fault could be at the subcritical state (cf. Atkinson, 1984; Main and  
51 Meredith, 1989) before its failure occurs. Hence, it is still significant to explore an  
52 acceptable, workable model for predicting the failure time,  $t_f$ , the magnitude,  $M$ , and  
53 the source area of a forthcoming earthquake from observed precursors, especially for  
54 a single fault.

55 Although reliable precursors may provide us a clue to judge whether or not an  
56 earthquake will happen in an area, the observations of precursors that are merely on  
57 the reduction side of science (see Kuhn, 1962) thus cannot be directly applied to  
58 predict anything. Hence, earthquake scientists need workable theories or models,  
59 which are on the deduction side, for prediction. Up to date, the reduction side is much  
60 stronger than the deduction one on the earthquake prediction research. This cannot  
61 make earthquake prediction be successful. A major effort is still needed in the

You will immediately lose a large number of readers, with such an opening sentence. Although some papers (mostly from the 1970's to 1990's) explore possible precursory signals, evidence is variable at best, controversial certainly. It is a huge leap to extend from a few studies of selected earthquakes, to stating that large earthquakes are "usually" preceded by precursory processes and (by implication) by observable precursors.

This begins a more reasonable discussion of the fact that earthquake prediction is debatable. Presenting the topic in a fair and balanced way does not detract from the purpose of the paper.

This is a good point.



62 scientific community in order to advance physical theories and models towards the  
63 great goal of earthquake prediction. One of the most important matters is  
64 the construction of physico-chemical models for respective precursors or even a  
65 unified model for all precursors. Through the comparison between the observations  
66 and the models, earthquake scientists could obtain the optimum ones for respective  
67 precursors or the optimum unified one. Based on the optimum models or the optimum  
68 unified one, earthquake scientists may be capable of predicting an earthquake,  
69 including its location, time window, and magnitude as mentioned above. Of course,  
70 such a model could be region-dependent, because different tectonic and geological  
71 conditions will influence the parameters of the model.

72 Reid's elastic rebound theory (Reid, 1910) assumes that the loading stress and slip  
73 on a fault are the major factors in causing an earthquake rupture. Numerous authors  
74 (e.g., Dieterich, 1978; Lomnitz and Lomnitz-Adler 1981; Kostrov and Das, 1982;  
75 Main, 1988, 1999; Scholz, 1990) assumed that the pre-seismic stress,  $\sigma$ , and slip,  $u$  (or  
76 strain,  $\varepsilon$ ), on a fault are two important factors in influencing the generation of  
77 precursors. Anomalous pre-seismic displacements or strains near the faults have been  
78 observed before numerous earthquakes. Tsubokawa et al. (1964) first measured  
79 pre-seismic displacements at several inland sites before the June 16 1964 M7.5  
80 Niigata, Japan, earthquake. Kanamori (1973, 1996) reported pre-seismic release  
81 associated with forthcoming major earthquakes, especially in Japan. Yu et al. (2001)  
82 reported the pre-seismic displacements on the near-fault stations before the September  
83 20 1999 M7.6 Chi-Chi, Taiwan, earthquake. Papazachos et al. (2002) found  
84 accelerating pre-seismic crustal deformation before large earthquakes in the Southern  
85 Aegean area. Sarkar (2011) observed possible accelerated Benioff strains prior to  
86 large earthquakes in the Sistan Suture Zone of Eastern Iran. These studies confirm the  
87 significance and importance of pre-seismic slip or strain on either earthquake  
88 prediction or assessment for forthcoming earthquakes. These studies confirm the  
89 significance and importance of pre-seismic slip or strain on earthquake prediction or  
90 assessment of forthcoming earthquakes.

91 Laboratory experiments reveal that  $\sigma$  and  $u$  are time-varying (Atkinson, 1984;  
92 Rudnicki, 1988; Main and Meredith, 1989). While, the slip as well as the strain  
93 increased very slowly with time from the initial time  $t_0$  to a particular time  $t_c$  and then  
94 increased rapidly from  $t_c$  up to the failure time  $t_f$  when an earthquake happens This is

Many of the cited papers are of the "reductionist" type. The author could do a service by pointing this out, or pointing to some examples of this among the many papers he cites. And also to some papers that follow the more-desired deductive approach.

It is disingenuous to neglect to mention that many (more?) studies have failed to identify precursory strains, displacements, or anything else before earthquakes. This sets a biased tone for the entire paper.

These selected studies do not "confirm" the claimed points. They are suggestive, and were among those that prompted a great deal of careful observational work that largely failed to confirm the existence of observable precursors.

By not acknowledging decades of work, large bodies of literature, negative findings, and alternative hypotheses, the author risks relegating this paper to join others in a "fringe" view of earthquake physics, a "true-believer" category.



the so-called quasi-static subcritical crack growth (SCG) model (Atkinson, 1984, 1987; Atkinson and Meredith, 1987) which is usually represented by the Charles law (e.g., Das and Scholtz, 1981; Main, 1988, 1999). Das and Scholz (1981) used this model with Charles law to describe the acceleration of a crack tip from an initially slow (sub-critical) rate due to stress corrosion to rapid remarkable rupture under increasing stresses. They predicted the failure time which depends on initial conditions on a fault, such as crack length, crack-tip velocity, residual frictional stress following a previous earthquake, stress-corrosion index, and the rate of stress input. Main (1988) applied a similar theory to predict the occurrence time of an event. His model may quantitatively explain the decrease of failure time in the crust in terms of decreases in the residual stress due to increasing heat flow, coupled with increases in both stress-input rates and density of nucleation points for rupture initiation. The model also predicts progressively increasing failure times for normal, strike-slip, and thrust faults under similar conditions. Wang (2021a,b; 2023) and Wang et al. (2016) classified the long-term, intermediate-term, short-term, and immediate-term precursors based on the SCG (subcritical crack growth) model as mentioned above.

From rock mechanic experiments, Voight (1988, 1989) proposed a nonlinear rate-dependent law for material failure:

$$X_{tt} - \alpha X_t^{-\alpha} = 0 \quad (1)$$

where  $X$  is an observable quantity,  $X_{tt}$  and  $X_t$  denote  $d^2X/dt^2$  and  $dX/dt$ , respectively,  $\alpha$  is a constant, and  $\alpha$  is the scaling exponent of the model. Based on rock mechanics,  $X$  may be interpreted in terms of conventional geodetic observations (e.g., length change, fault slip, strain or angular change), seismic quantities (e.g., the square root of cumulative energy release or Benioff strain) or geochemical observations (such as gas emission rates or chemical ratios). The parameter  $\alpha$  varies with rock materials and also depends on the temperature. Eq. (1) is called the Voight's equation hereafter. Some authors (e.g., Varnes, 189; Kilburn and Voight, 1998) compared Eq. (1) with the Charles law for the SCG model. Essentially, the Voight's equation is similar to the Charles law. The Voight's equation has been applied to predict the failure time of an earthquake based on the accelerated Benioff strain (e.g., Bufe and Vanus, 1993; Bowman et al., 1996) and the accelerating strain (e.g., Main, 1999). In addition, Main

Rewording needed:  
Laboratory observations are not a model. Atkinson and Meredith applied the SCG model to the laboratory data.

Which model? (Several have been mentioned in preceding sentences.)



(1999) also studied the failure times of earthquakes by considering constitutive rules of a simple percolation model (e.g., Stauffer and Aharony, 1994). However, they did not predict the magnitude of a forthcoming earthquake.

The pre-seismic strains observed on or near a fault are directly related to the stress and slip on the fault zone. Define  $T=t_f-t_0$ , where  $t_0$  is the initial occurrence time of the precursor, be the precursor time (see Wang et al., 2016; Wang, 2021a,b). In this study, we will propose a theory to predict the failure time,  $t_f$ , magnitude,  $M$ , and location of a forthcoming earthquake and to investigate the relationship between the precursor time and earthquake magnitude from the pre-seismic and co-seismic strains based on the Voight's equation. In addition, the theory can be also applied to other kinds of precursors.

## 2 Voight's Equation

From the results obtained from the rock mechanics experiments, Voight (1988) proposed the empirical equation, i.e., the so-called Voight's equation, to describe rate-dependent material failure. The Voight's equation has been considered as a fundamental physical law governing diverse forms of material failures (e.g. Voight, 1988, 1989). It is a more general form of Charles' law (Main, 1999). Like several authors (e.g., Das and Scholtz, 1981; Main, 1988, 1999), I assume that this empirical equation can be applied to real earthquakes. In addition, this empirical equation has been applied to volcanic eruptions (Voight, 1988b; Cornelius and Voight, 1995; Kilburn and Voight, 1998).

If  $X$  in Eq. (1) is taken to be the strain,  $\varepsilon$ , on a fault, the final stages of failure under steady conditions of a rock in compression would show a proportionality between the logarithm of creep acceleration and the logarithm of creep velocity. Integrating Eq. (1) gives the expression for the strain rate,  $\dot{\varepsilon}_t$ , and strain acceleration,  $\ddot{\varepsilon}_t$ , on a fault zone. In the followings, the strain and strain rate at the initial time,  $t_0$ , are denoted by  $\varepsilon_0$  and  $\dot{\varepsilon}_{t_0}$ , respectively; while those at the failure time,  $t_f$ , are shown by  $\varepsilon_f$  and  $\dot{\varepsilon}_{t_f}$ , respectively. The solution is dependent on the scaling exponent  $\alpha$ . For  $\alpha=1$ , the strain rate is

$$\dot{\varepsilon}_t = \dot{\varepsilon}_{t_0} e^{\alpha(t-t_0)}. \quad (2)$$

In the introduction, the author notes that complexity may get in the way of precursor development. It is worth considering how much of this subsequent development is likely to apply to a complex (e.g., non-planar) fault in a complex (e.g., inhomogeneous) crustal setting. Detailed studies of earthquakes—possible in the past 20 years due to dense seismic and geodetic recording—show faults and earthquakes to be extremely complex at all scales studied.



161

162 For  $\alpha < 1$ , the strain rate is

163

$$\varepsilon_t = [a(1-\alpha)(t-t_o) + \varepsilon_{to}^{(1-\alpha)}]^{1/(1-\alpha)}. \quad (3)$$

165

166 For  $\alpha > 1$ , the strain rate is

167

$$\varepsilon_t = [a(\alpha-1)](t_f-t) + \varepsilon_{tf}^{(1-\alpha)}]^{1/(1-\alpha)}. \quad (4)$$

169

170 These equations remarkably reveal that  $\varepsilon_t$  increases with time and thus there is not an  
171 upper bound of  $\varepsilon_t$ . The value of  $\varepsilon_t$  can be evaluated from the first two equations for  
172  $\alpha \leq 1$  and cannot be resolved from the third equation for  $\alpha > 1$ . It seems that there is a  
173 singular point at  $t_f$  for  $\alpha > 1$ . At the singular point, a rock fracture or an earthquake  
174 would happen. An example of numerical results can be seen in Voight's (1989) Figure  
175 2. Since  $\varepsilon$  is integrated from  $\varepsilon_t$ , there is not an upper bound value for  $\varepsilon$  when  $\alpha \leq 1$ .

176 We may further solve the time-dependent strain  $\varepsilon(t)$  through double integration of  
177 Eq. (1). For  $\alpha > 1$  and  $\alpha \neq 2$ , the result is

178

$$\varepsilon(t) - \varepsilon_o = \{ [a(\alpha-1)(t_f-t_o) + \varepsilon_{tf}^{(1-\alpha)}]^\eta - [a(\alpha-1)(t_f-t) + \varepsilon_{tf}^{(1-\alpha)}]^\eta \} / a(\alpha-2) \quad (5)$$

180

181 where  $\eta$  represents  $(2-\alpha)/(1-\alpha)$ . For  $\alpha > 1$  and  $\alpha \neq 2$ , the values of  $\eta$  are: (1)  $\eta < 0$  as  
182  $1 < \alpha < 2$ ; and (2)  $\eta > 0$  as  $\alpha > 2$ . From the theoretical studies made by Main (1998), we  
183 can see that the condition of the existence of accelerating strain for generating an  
184 earthquake is  $1 < \alpha < 2$ , thus leading to  $\eta < 0$ . This condition will be used hereafter.

185

### 186 3. Theory of earthquake prediction

187

188 According to the Voight's equation, I assume that it is possible to predict the failure  
189 time of a forthcoming earthquake from the observed pre-seismic strains measured on  
190 or near the fault along which the event will occur. The prediction of the failure time is  
191 based on Eq. (4) and the prediction of the magnitude is based on Eq. (5). The location  
192 of the event should be near the sites of observing the pre-seismic strains. The theory



193 of earthquake prediction proposed in this study is described below.

194

### 195 **3.1 Predicting the Failure Time of a Forthcoming Earthquake**

196

197 Since the condition  $1 < \alpha < 2$  is considered here, we will only take Eq. (4) in the  
198 followings. Due to  $1 - \alpha < 0$ , the strain rate,  $\varepsilon_t$ , at the failure time should be much larger  
199 than 1 strain/sec and thus  $\varepsilon_t^{1-\alpha}$  is much smaller than 1 strain/sec. This makes Eq. (4)  
200 become

201

$$202 \quad \varepsilon_t = [a(\alpha - 1)(t_f - t)]^{1/(1-\alpha)}. \quad (6)$$

203

204 The time variations in  $\varepsilon_t$  from Eq. (6) for  $\alpha = 1.5, 1.6$ , and  $1.7$  when  $a = 0.5$  are  
205 displayed in Fig. 1 in which  $\varepsilon_t$  is normalized by the maximum value of  $\varepsilon_t$  for the three  
206 cases. In the figure, the three curves intersect to one another at a point with  $t = t_c$ .  
207 When  $t < t_c$ ,  $\varepsilon_t$  increases slowly with time and increases with  $\alpha$ ; while when  $t > t_c$ ,  $\varepsilon_t$   
208 increases rapidly with time and decreases with increasing  $\alpha$ .

209 From Eq. (6), we propose a method to explore the possibility of predicting the  
210 failure time,  $t_f$  of a forthcoming earthquake. Since the values of three model  
211 parameters  $t_f$ ,  $a$ , and  $\alpha$ , must be solved, those of  $\varepsilon_t$  at three time instants should be  
212 given. Considering the pre-seismic strain rates, i.e.,  $\varepsilon_{t1}$ ,  $\varepsilon_{t2}$ , and  $\varepsilon_{t3}$ , at three time  
213 instants, i.e.,  $t_1$ ,  $t_2$ , and  $t_3$ , respectively. An example for  $\alpha = 1.6$  with  $a = 0.5$  is shown in  
214 Fig. 2 in which  $\varepsilon_t$  is normalized by the maximum value of  $\varepsilon_t$ . Inserting  $\varepsilon_{tj}$  and  $t_j$  ( $j = 1,$   
215  $2$ , and  $3$ ) into Eq. (6) yields

216

$$217 \quad \varepsilon_{tj} = [a(\alpha - 1)(t_f - t_j)]^{1/(1-\alpha)} \quad (j = 1, 2, 3). \quad (7)$$

218

219 This leads to

220

$$221 \quad t_f = t_j + \varepsilon_{tj}^{(1-\alpha)/a} / a(\alpha - 1) \quad (j = 1, 2, 3). \quad (8)$$

222

223 From Eq. (8) for  $\varepsilon_{t1}$  at  $t_1$  and  $\varepsilon_{t2}$  at  $t_2$ , we have

224

Much is made of  $1 < \alpha < 2$ , but tell us more about what  $\alpha$  represents. Has it been estimated for rocks or the crust? Has it been shown to lie between 1 and 2 for conditions likely to exist on or around faults in the crust?

Same questions for constant  $a$ , which is later used (e.g., assumed  $a = 0.5$ ).

Alpha can range from 1 to 2. Why is the narrow range 1.5-1.7 chosen to illustrate the model behavior in the figures?



$$t_2 - t_1 = [\varepsilon_{i2}^{(1-\alpha)} - \varepsilon_{i1}^{(1-\alpha)}] / a(\alpha - 1) \quad (9a)$$

226

227 or

228

$$a(\alpha - 1) = [\varepsilon_{i2}^{(1-\alpha)} - \varepsilon_{i1}^{(1-\alpha)}] / (t_2 - t_1). \quad (9b)$$

230

231 Similarly, from Eq. (8) for  $\varepsilon_{i1}$  at  $t_1$  and  $\varepsilon_{i3}$  at  $t_3$  we have

232

$$t_3 - t_1 = [\varepsilon_{i3}^{1/(1-\alpha)} - \varepsilon_{i1}^{1/(1-\alpha)}] / a(\alpha - 1) \quad (10a)$$

234

235 or

236

$$a(\alpha - 1) = [\varepsilon_{i3}^{(1-\alpha)} - \varepsilon_{i1}^{(1-\alpha)}] / (t_3 - t_1). \quad (10b)$$

238

239 Define two functions in term of  $\alpha$ , i.e.,  $F_{21}(\alpha) = [\varepsilon_{i2}^{(1-\alpha)} - \varepsilon_{i1}^{(1-\alpha)}] / (t_2 - t_1)$  and  $F_{31}(\alpha) =$

240  $[\varepsilon_{i3}^{(1-\alpha)} - \varepsilon_{i1}^{(1-\alpha)}] / (t_3 - t_1)$ . From Eqs. (9b) and (10b),  $F_{21}(\alpha)$  and  $F_{31}(\alpha)$  are the same

241 because they are both equal to  $a(1-\alpha)$ . We may evaluate the value of  $\alpha$  directly from

242 the equality  $F_{21}(\alpha) = F_{31}(\alpha)$ . We first plot the difference of the two functions for

243  $1 < \alpha < 2$ . An example of  $F_{21}(\alpha) - F_{31}(\alpha)$  in terms of  $\alpha = 1.6$  is shown in Fig. 3 in which

244 the normalized values of  $F_{21}(\alpha) - F_{31}(\alpha)$ , i.e.,  $(F_{21}(\alpha) - F_{31}(\alpha)) / (F_{21}(\alpha) - F_{31}(\alpha))_{\max}$ , is

245 given. The condition for the existence of the value of  $\alpha$  to make  $F_{21}(\alpha) = F_{31}(\alpha)$  is that

246 the curve of  $F_{21}(\alpha) - F_{31}(\alpha)$  must intersect the horizontal line with  $F_{21}(\alpha) - F_{31}(\alpha) = 0$  at

247 a point with a certain value of  $\alpha$  as displayed in Fig. 3. After the value of  $\alpha$  has been

248 evaluated, we may calculate the value of  $a$  from either  $a = F_{21}(\alpha) / (1-\alpha)$  or  $a = F_{31}(\alpha) /$

249  $(1-\alpha)$ . Then, we may evaluate the failure time of the forthcoming earthquake from Eq.

250 (7) by using the following expression:

251

$$t_f = t_j + \varepsilon_{ij}^{1/(1-\alpha)} / a(\alpha - 1) \quad (j=1, 2, 3). \quad (11)$$

253

254 The difference between the occurrence time of a precursor and the failure time of the

255 forthcoming earthquake is called the precursor time (e.g., Wang et al., 2016; Wang,

256 2021a,b) and is denoted by  $T$  hereafter. For the present case, the occurrence time of

Give us a sense of what  
F21 and F31 represent.

What does this mean? Are  
you using Figure 3 to  
discover the appropriate  
value of alpha?





the precursor and the failure time of the forthcoming earthquake are  $t_o$  and  $t_f$ , respectively, thus leading to  $T=t_f-t_o$ .

### 3.2 Prediction of the Magnitude of a Forthcoming Earthquake

Based on the evaluated precursor time,  $T$ , it is possible to predict the magnitude of an earthquake by using Eq. (5). It first needs to discuss the value of initial strain  $\varepsilon_o$ . After the ruptures of last earthquake on a fault, the fault usually continues to slide with the relative movement speed of regional plates until the occurrence of the next event. If the moving speed is  $v_p$ , the strain rate,  $\varepsilon_t$ , is  $v_p/L$  where  $L$  is the fault length on a fault. Here the value of  $\varepsilon_t \delta t$  with the time unit  $\delta t$  of 1 second is taken to be  $\varepsilon_o$ . The value of  $\varepsilon_t$  is commonly  $10^{-6}$  strain/year around the world (e.g., Scholz et al., 1973; Turcotte and Schubert, 1982; Yu et al., 2001). For an example, the value of  $\varepsilon_t$  is  $0.25 \times 10^{-6}/\text{yr} = 1.90 \times 10^{-13}/\text{sec}$  for the San Andres fault (cf. Turcotte and Schubert, 1982), thus leading to  $\varepsilon_o = 1.90 \times 10^{-13}$  which is much smaller than 1. This makes us able to take  $\varepsilon_o = 0$  in this study. Figures 1 and 2 reveal  $\varepsilon_{tf} \gg 1$ . According to the two conditions, Eq. (5) becomes

$$\varepsilon(t) = \{[a(\alpha-1)T]^\eta - [a(\alpha-1)(t_f-t)]^\eta\} / a(\alpha-2). \quad (12)$$

Voight (1988, 1989) took  $a=0.5$  for studying the results of his rock mechanic experiments. Hence, the values of  $\varepsilon_t$  is about a few strain/day or  $10^{-4}$  strain/sec for laboratory earthquakes. As mentioned above, the values of pre-seismic strain,  $\varepsilon$ , much before the occurrences of natural earthquakes are very small. Hence, the value of parameter  $a$  should be small for natural earthquakes. Nevertheless, the value of  $a$  is still taken to be 0.5 in Fig. 4 which illustrates the time variations in  $\varepsilon$  from Eq. (12) for  $\alpha=1.5$ , 1.6, and 1.7. In the figure,  $\varepsilon$  is normalized by the maximum value of the three cases. Like Fig. 1, Fig. 4 shows that the three curves intersect to one another at a point with  $t=t_c$ . When  $t < t_c$ ,  $\varepsilon_t$  increases slowly with time and increases with  $\alpha$ ; while when  $t > t_c$ ,  $\varepsilon_t$  increases rapidly with time and decreases with increasing  $\alpha$ .

The earthquake ruptures at  $t=t_f$  when the strain is  $\varepsilon_f$ , which is

Why not use a realistic value of  $a$ , rather than  $a=0.5$ ? This does not convince us that the treatment has relevance to the real world.



$$\varepsilon_f = [a(\alpha-1)T]^\eta / a(\alpha-2) \quad (13)$$

290

291 from Eq. (12). This is the upper bound of  $\varepsilon(t)$  for  $\alpha > 1$  and  $\alpha \neq 2$ . This upper bound is

292 dependent on both the parameters of fault-zone materials and precursor time.

293 Re-organizing Eq. (13) and taking the logarithm on the two sides of the re-organized

294 equation yield

295

$$\log(T) = \log\{[a(\alpha-2)\varepsilon_f]^{1/\eta} / [a(\alpha-1)]^\eta\}. \quad (14)$$

297

298 Eq. (14) gives

299

$$\log(T) = \log\{[a(\alpha-2)]^{1/\eta} / a(\alpha-1)\} + \log(\varepsilon_f) / \eta. \quad (15)$$

301

302 This represents the power-law scaling relationship between  $T$  and  $\varepsilon_f$ , i.e.,  $T \sim \varepsilon_f^{1/\eta}$ .

303 Since the rupture duration of an earthquake is short, we may consider  $\varepsilon_f$  as the

304 average strain over the ruptured area after failure. Shaw (2023) inferred the scaling

305 law for  $\varepsilon_f$  versus the fault length of an earthquake,  $L$ , in the following form:  $\varepsilon_f = \lambda L^{-1/2}$ .

306 This leads to

307

$$\log(\varepsilon_f) = \log(\lambda) - \log(L)/2, \quad (16)$$

309

310 where  $\lambda$  is a region-dependent constant. Several authors (e.g., Kanamori and

311 Anderson, 1976; Wells and Coppersmith, 1994; Leonard, 2010; Thingbaijam et al.,

312 2017; Wang, 2018; Shaw, 2023) inferred the scaling law for  $L$  versus  $M$ , which is the

313 earthquake magnitude (usually the seismic-wave magnitude,  $M_s$ , or the moment

314 magnitude,  $M_w$ ), in the following form:

315

$$\log(L) = \chi + M/2 \quad (17)$$

317

318 where  $\chi$  is a constant depending on tectonic and geological conditions. Combination

319 of Eqs. (15), (16), and (17) leads to the  $\log(T)$ - $M$  relationship:

320

$$\log(T) = C + AM \quad (18)$$

321

Here, as elsewhere, it would be helpful to provide an estimate of e-sub-f (the strain at initiation of failure) for reasonable values of  $a$ ,  $\alpha$ ,  $\eta$  and  $T$ .

How do those estimates of e-sub-f compare to the observational limits that we have on precursory strain? Many geodetic studies (including at Parkfield) have shown that precursory strain (if any) is below the detectable limit.

In other words, is the author's analysis in line with current observational data? If so, this is encouraging (though will emphasize that precursory strain should be hard to detect). If not, the author should comment on this point, and provide arguments for why we should trust the following points in his analysis.

Tell us the expected range of values for this constant. Then calculate some examples for the expected values of e-sub-f, given this range of the constant and the length  $L$  of large- $M$  earthquake ruptures (e.g., hundreds of meters to tens of kilometers).

Again, tell us the expected range of this constant.



322

323 where two new parameters are  $C = \log\{[a(\alpha-2)]^{1/\eta}/a(\alpha-1)\} + [\log(\lambda) - \chi/2]/\eta$  and  $A = -1/4\eta$ .

324 Obviously,  $A$  is positive due to  $\eta < 0$  because of  $1 < \alpha < 2$  as mentioned above. This

325 results in a positive correlation between  $T$  and  $M$ . When  $T$  is known, the value of  $M$

326 for the forthcoming earthquake may be evaluated from Eq. (18), i.e.,  $M = [\log(T) - C]/A$ .

327 From past studies (cf. Wang, 2021b, 2023; and cited references therein), the values of

328  $A$  from observations are all smaller than 1. This leads to  $\alpha < 1.8$  and thus the values of

329  $\alpha$  for natural earthquakes could be in the range 1.0 to 1.8.

330

### 331 3.3 Predicting the Location of a Forthcoming Earthquake

332

333 As mentioned by Aki (1989), the earthquake scientists should provide the location of

334 the forthcoming earthquake to the public. Hence, predicting the potential location of

335 the forthcoming earthquake is also important for seismic hazard mitigation. When the

336 stations on which the pre-seismic strains are observed are close to a known active

337 fault, it is very possible to assess the occurrence of the forthcoming earthquake along

338 the fault. On the other hand, when the station site is not close to a known active fault

339 or within a complicated active fault system, it needs other precursors, for example,

340  $b$ -value anomalies (e.g., Wang et al., 2016), foreshock activities (e.g., Chen and Wang,

341 1984; Chen et al., 1990; Gulia and Wiemer 2019; Zaccagnino et al., 2024),

342 geochemical anomalies (e.g., Walia et al., 2009; Fu and Lee, 2018) electromagnetic

343 anomalies (e.g., Ohta et al., 2005, Hayakawa et al., 2006; Hayakawa and Hobara,

344 2010; De Santis et al., 2019) etc., for helping earthquake scientists to make correct

345 assessment. Hence, researchers have also suggested other methods to judge the

346 possible location of the forthcoming earthquake. Seismologists (e.g., Rundle et al.,

347 2000; Wu et al., 2012) suggested a method to assess the location from seismicity

348 pattern. For some strike-slip and normal earthquakes, seismologists can assess the

349 possible location of the mainshock from its foreshocks (e.g., Chen et al., 1990).

350 Geochemists (e.g., Walia et al., 2009; Fu and Lee, 2018) suggest a method just like

351 that used by seismologists to locate an earthquake from the differences between travel

352 times of  $P$ - and those of  $S$ -waves recorded at three stations. They took the occurrence

353 times of geochemical precursors, recorded at three different stations to evaluate the

354 optimal location of a forthcoming earthquake. Geophysicists (e.g., Ohta et al., 2005,

Parameters  $A$  and  $C$  turn out to be important, and are given some discussion later in the paper. But nothing is said (here or there) about their meaning or physical interpretation. Please don't expect the reader to fight through the definition of  $C$  to gain that insight!

If I'm following correctly, if  $\alpha$  and  $a$  are known, one can estimate  $T$  from the previous section 3.2.

This is one of the few places where the author mentions that a complex fault system may provide greater challenges to prediction.

This is possible IF (and only if) there are precursory strains large enough to detect on those nearby instruments.

If precursory strain is related to the future earthquake  $M$ , stations must be located near that future fault rupture. However, if precursory strain is related to a localized process located near the future hypocenter, stations must be located close to that location. This was the entire observational strategy of the Parkfield earthquake prediction experiment.



Hayakawa et al., 2006; Hayakawa and Hobara, 2010) suggest the goniometric method to assess the location of the forthcoming event by detecting the directions of ULF emissions from the observational stations to the earthquake epicenter. These methods seem acceptable.

What does this mean? How is the author evaluating the “acceptability” of these hypotheses? Is he relying on his own intuition, or some theoretical arguments, or on published work that tested the hypotheses using real data?

## 4 Discussion

### 4.1 On the Theory for the Pre-seismic Strains

Fig. 1 shows that the strain rate,  $\varepsilon_t$ , monotonically increases with time. From Fig. 1, Eq. (1) will lead to an increase in the strain acceleration,  $\varepsilon_{tt}$ , with time. For the time variation as displayed in Fig. 1, at a certain time instant, larger  $\alpha$  yields higher  $\varepsilon_t$ . Meanwhile, there are two steps more or less separated at a particular time instant,  $t_c$ , which is shorter than  $t_f$  and not displayed in the figure. The two steps are:  $\varepsilon_t$  first slowly with time when  $t < t_c$  and then rapidly with time when  $t > t_c$ . Such a particular time appears earlier for large  $\alpha$  than for small  $\alpha$ . The second step is the existence of accelerating strain before a forthcoming earthquake from the theoretical studies by Main (1998). From observations of foreshocks, some authors (e.g., De Santis et al., 2015; and Cianchini et al., 2020) applied the revised accelerated moment release model to foreshocks revealing an acceleration pointing to the mainshock. Their model is similar to the present one. Since there is background noise in practical observations, the anomalous strain rate can be measured only in the second step. Like Fig. 1, Fig. 4 also illustrates the similar time variation in the strain,  $\varepsilon$ . For all cases in Fig. 4, there are also two steps separated at a particular time instant,  $t_c$ :  $\varepsilon$  first slowly with time when  $t < t_c$  and then rapidly with time when  $t > t_c$ . Unlike Fig. 1, such a particular time is almost the same for all  $\alpha$ 's in use. Meanwhile, in Fig. 4  $\varepsilon$  increases with  $\alpha$  when  $t$  is smaller than such a particular time; while  $\varepsilon$  decreases with increasing  $\alpha$ , when  $t$  is larger than such a particular time. This is the main difference between Fig. 1 and Fig. 4. In addition, larger  $\alpha$  produces lower  $\varepsilon_t$  as  $t$  is approaching  $t_f$  in Fig. 4. This means that the strain during a forthcoming earthquake increases with decreasing  $\alpha$ .

Missing word?

This statement is of questionable value without evaluating the level of “background noise” relative to expected amplitudes of anomalous strain during the two hypothesized steps. On what basis does the author conclude that the strain during the first step is below the “background noise” limit, and the strain during the second step is above that limit?

The theory of predicting the failure time of a forthcoming earthquake proposed by this study is basically similar to that used by Das and Scholz (1981) based the Charles



387 law and that suggested by Main (1988) based on the Voight equation. One difference  
388 between this method and theirs is that the values of strain rate at three time instants  
389 are taken in this study, while only those of pre-slip at two time instants were  
390 considered in theirs. This is due to a reason that they assumed that the model  
391 parameters of either Charles law or Voight's equation have been already known,  
392 while those in this study are originally unknown and must be estimated from the  
393 observations.

394 Equation (18) exhibits the  $\log(T)$ - $M$  relationship based on pre-seismic strains.  
395 Tsubokawa (1969, 1973) first obtained a linear relation between the precursor time of  
396 crustal movement and mainshock magnitude for Japanese earthquakes in the form:  
397  $\log(T) = -1.88 + 0.79M$ , with  $C = -1.88$  and  $A = 0.79$ . His observations somewhat confirm  
398 the existence of the  $\log(T)$ - $M$  relationship. This makes us capable of predicting the  
399 magnitude of a forthcoming earthquake when the precursor time has been evaluated  
400 from observations. Although the earthquakes used by Tsubokawa (1969, 1973)  
401 occurred on different fault zones, his  $\log(T)$ - $M$  relationship with the values of  $C$  and  
402  $A$  represents the average characteristics of crustal deformations in Japan. In general,  
403 the parameters  $a$  and  $\alpha$  of Voight's equation and  $\lambda$  and  $\chi$  of the scaling laws of faults  
404 vary from area to area. Hence, the  $\log(T)$ - $M$  relationships might be distinct in  
405 different fault systems.

406 Wang (2023) correlated the precursor time to the earthquake energy. The  
407 Gutenberg-Richter's energy-magnitude law of earthquakes (Gutenberg and Richter,  
408 1942, 1956) is:  $\log(E_s) = 11.8 + 1.5M$  in which  $E_s$  is the seismic-wave energy (in ergs)  
409 and  $M$  is commonly the surface-wave magnitude,  $M_s$ . From the law, he obtained the  
410 correlation:  $M \sim (2/3)\log(E_s)$ . In addition, from  $\log(T) = C + AM$  he got  $\log(T) \sim AM \sim$   
411  $(2A/3)\log(E_s)$ . Since  $E_s = \xi \Delta E$  where  $\Delta E$  is the strain energy of an earthquake and  $\xi$   
412 ( $< 1$ ) is the seismic efficiency, Wang (2004) obtained  $T \sim \Delta E^{A\xi/3}$ . This indicates that the  
413 precursor time is dependent on the strain energy of the forthcoming earthquake. The  
414 seismic efficiency that depends on the physical and chemical properties of the  
415 fault-zone rocks (Knopoff, 1958; Kanamori and Heaton, 2000; Wang, 2009) may also  
416 influence  $T$ . A high seismic efficient will yield a long precursor time.

## 418 4.2 Application of the Theory to Other Earthquake Precursors

419

Using practical observations, how may the necessary parameters be estimated? Guidance would be helpful (perhaps provided in the following sections).

If practical means exist to estimate the parameters, why does the author not do so using some examples of well-recorded earthquakes? Or can he point to any studies in which this was done in the 3-4 decades since those theoretical papers were published?

Again, provide some example calculations: for reasonable estimates of seismic efficiency, what values of  $T$  are expected for various large  $M$ 's?

The value of seismic efficiency has been estimated in many papers. Provide a reasonable range.

Help the reader: what are the units of  $A$  and  $C$ , and what units of  $T$  are computed (seconds?).

Assuming that these values of  $A$  and  $C$  are correct for Japan, compute the precursory time  $T$  for various magnitudes of Japanese earthquakes. Also, use the analysis above to estimate the amplitude of precursory strain expected for various earthquake magnitudes.

Japan has the world's best geodetic monitoring system. Are those levels of precursory strain large enough to be detected by the current geodetic network? If so, have they been detected, or not?



#### 4.2.1 The $\log(T)$ – $M$ relationships for other Precursors

421

422 In order to measure the pre-seismic strains, the strain-meters should be installed on or  
423 **much near** the fault. When a strain-meter has not installed on or near the fault on  
424 which a forthcoming earthquake will happen, it is hence necessary to use other kinds  
425 of precursors which are directly or indirectly caused by the pre-seismic fault slip or  
426 strains for predicting the earthquake. In other word, it is **much significant** to explore  
427 the application of the present theory on the prediction of  $t_f$  and  $M$  of a forthcoming  
428 earthquake based on other kinds of precursors in practice. The present theory can be  
429 applied to other kinds of precursors, and thus the  $\log(T)$ – $M$  relationships exist for  
430 these precursors. It is significant to apply the above-mentioned theory to predict the  
431 failure time and magnitude of a forthcoming earthquake based on other kinds of  
432 precursors.

433 The  $\log(T)$ – $M$  relationships have been recognized from the observations of  
434 different kinds of precursors for a long time (Rikitake 1975a; Wang, 2021a,b, 2023;  
435 and cited references therein). **From** the plot of  $T$  (in days) versus  $M$  for five precursors,  
436 i.e., crustal movements, electric resistivity, radon (denoted as Rn hereafter) emission,  
437  $v_p/v_s$  anomaly, and  $b$ -value of Gutenberg-Richter frequency-magnitude law  
438 (Gutenberg and Richter, 1944). From 30 world-wide earthquakes, Scholz et al. (1973)  
439 inferred a relationship:  $M_s = -5.81 + 1.55 \log(T)$  ( $T$  in days) or **Correct???**  $\log(T) = 3.75 + 0.65 M_s$ . For  
440 the precursors of crustal deformations and seismic-wave velocities, Whitcomb *et al.*  
441 (1973) obtained  $\log(T) = -1.92 + 0.80 M_s$  ( $T$  in days). Rikitake (1975b) obtained  $\log(T) =$   
442  $-1.83 + 0.76 M_s$  ( $T$  in days). He also stressed that the  $\log(T)$ – $M_s$  relationships are  
443 different for different groups of precursors. Rikitake (1979, 1984) divided a large data  
444 set of 391 cases of precursors into three classes. He obtained **T in days or years?**  $\log(T) = -1.01 + 0.60 M_s$  for  
445 the first class including 192 cases and **No dependence on  $M$ ?**  $\log(T) = -1.0$  for the second class. He did not  
446 report any relationship for the third class for foreshocks, tilt and strain, and earth's  
447 currents. Smith (1981, 1986) obtained the following  
448 relationship:  $\log(T) = 1.42 + 0.30 M_s$  ( $T$  in years) from the data of abnormal  $b$ -values for  
449 earthquakes in New Zealand. Ding et al. (1985) obtained  $\log(T) = -0.34 + 0.38 M_s$  ( $T$  in  
450 years) for various precursors proceeding large Chinese earthquakes. From the  $b$ -value  
451 anomalies for 45 world-wide earthquakes with  $3 \leq M_s \leq 9$ , Wang et al. (2016) obtained  
452  $\log(T) = (2.02 \pm 0.49) + (0.15 \pm 0.07) M_s$  ( $T$  in years).

453 From the previous description, it is clear that the  $\log(T)$ – $M$  relationships are

The writing is generally quite clear, but the paper requires proofreading by a native english writer, to correct numerous small errors of grammar.

No verb in this sentence.

This paragraph summarizes findings from several papers. It should be straightforward for the author to provide a table of  $T$  for various values of  $M$ , for these studies.

For example, using the Scholz (1973) relation: for an earthquake of  $M_s = 6$ ,  $\log(T) = 3.75 + 0.65 \times 6 = 7.65$ .  $T = 4.47 \times 10^7$  days = 1,224 centuries. Is this a useful result?

For Whitcomb (1973) and  $M_s = 6$ ,  $T = 759$  days, which would be a more interesting hypothesis.





different for distinct kinds of precursors and also region-dependent. These results strongly suggest regional-dependence of  $C$  and  $A$  of Eq. (18). Clearly,  $C$  is influenced by several parameters, while  $A$  is controlled only by the scaling exponent,  $\alpha$ , of the fault-zone materials. Hence,  $A$  is an important indicator of the relationship. The previous studies lead to two interesting points. First, for the same forthcoming earthquake, different kinds of precursors may have different precursor times due to distinct values of  $C$ , but the same value of  $A$ . Secondly, for the forthcoming earthquakes that have the same magnitude and occur at different fault zones, different kinds of precursors may have different precursor times due to distinct values of both  $C$  and  $A$ .

We will explore the theoretical basis for two kinds of precursors in the followings. The first kind of precursors is the geoelectric signals which are yielded almost within the fault zone where the forthcoming earthquake will happen, and the other is the geochemical signals which might occur on the sites that are somewhat far away from the fault zone. The mechanisms to generate the two kinds of signals will be described below.

#### 4.2.2 For the Geoelectric Precursors

Changes or anomalies of geoelectric signals have been observed prior to earthquakes for a long time (cf. Hayakawa and Hobara, 2010; and cited references therein).

Geoelectric signals are associated with pre-seismic slip on a fault where a forthcoming earthquake will happen. It is necessary to build up a comprehensive model that presents the lithosphere-ocean-atmosphere-ionosphere-magnetosphere coupling to interpret the generation of geoelectric precursors (Potirakis et al., 2017; Ouzounov et al., 2018; and cited references therein). Several proposed models are: (1) a model to present  $R_n$  ionization and charged aerosol and change of load resistance in the global electric circuit (Ouzounov et al., 2018; Pulinets and Ouzounov, 2018; and cited references therein); (2) a model to show coupling between stressed rocks and the atmosphere-ionosphere system (e.g., Kuo et al., 2011, 2014) based on experimental results of stress-induced charges made by Freund (2002); (3) a model to display ionosphere dynamics with imposed zonal (west-east) electric field (Zolotov et al., 2011, 2012; Namgaladze et al., 2012); and (4) a model of leakage of electric currents

It would be helpful to provide the reader with insight into the significance or meaning of  $A$  and  $C$ . That help is not provided when  $A$  and  $C$  are defined, nor here. And note that this discussion section located far later than Eqn 18. Without that insight, the reader won't appreciate the comments that follow, which seem important.

Many studies have also failed to discover any EM anomalies prior to earthquakes.



from ocean into the crust having low electric resistivity (Madden and Mackie, 1996). The existence of electric charges/currents on the Earth's ground or in the uppermost crust is a necessary condition for these models. Several mechanisms, including microfracturing (e.g., Ogawa et al., 1985; Molchanov and Hayakawa, 1995), electrokinetic effect (e.g., Mizutani et al., 1976), streaming potentials (e.g., Bernard, 1992), piezoelectricity (e.g., Bishop, 1981; Sornette, 2001; Wang, 2021c), triboelectricity/triboluminescence (e.g., Yoshida et al., 1998), confined pressure changes (e.g., Fujinawa et al., 2002), the peroxy defect theory (Freund, 2002), piezomagnetism (e.g., Sasai, 1979, 1980; Martin, 1980), etc. have been proposed to explain electric charge generation within the fault zones.

Here, we show three examples to show the geoelectric and geomagnetic precursors caused by pre-seismic ground electric currents. First, Whitworth (1975) proposed a model of the motion of charged edge location (MCD). According to the MCD model, numerous authors (e.g., Tzanis and Vallianatos, 2002; Venegas-Aravena et al., 2019) assumed that an electric current density,  $J$ , generated within rocks under compressional stress changes with time, i.e.,  $\sigma_t = d\sigma/dt$ , can be represented by  $J = 2^{1/2}(q/\psi B_v)(\sigma_t/Y)$  where  $q$  is the linear charge density of edge dislocation,  $B_v$  is the Burgers vector module,  $\psi (=1-3)$ , which represents the dislocation number created by compression and uniaxial tension within a rock (Whitworth, 1975; Vaillianatos and Tzanis, 1998), and  $Y$  is the Young's effective module (Turcotte et al., 2003). Since the quantity  $\sigma_t/Y$  may be replaced by the strain rate  $\varepsilon_t$ , the electric current density becomes  $J = 2^{1/2}(q/\psi B_v)\varepsilon_t$ . The geoelectric field is  $E = J/\theta_c$ , where  $\theta_c$  is the electric conductivity, from the Maxwell equation. Meanwhile, the geomagnetic field at a distance,  $r$ , from the electric current density is  $|B| = \mu_B |J|/2\pi r$ , where  $\mu_B$  is the permeability of free space, from the Biot-Savart law (cf. Corson and Lorrain, 1962). Clearly,  $E$  and  $B$  are both related to  $\varepsilon_t$ . Secondly, Enomoto (2012) obtained  $\log(J) = 0.5M + \log(5.1 \times 10^2 e k n h^2 D_c / \nu)$  ( $e$ =the electronic charge;  $k$ =a constant of proportionality;  $n$ =the density of negatively charged gas molecules;  $h$ =the crack gap;  $D_c$ =critical depth; and  $\nu$ =the gas viscosity). This shows the correlation between  $J$  and  $\varepsilon$ . Thirdly, some authors (e.g., Sornette, 2001; Wang, 2021c) studied the dependence of ground electric field,  $E$ , on pre-seismic slip,  $u$ , in a fault zone in a one-dimensional model with the spatial coordinate  $x$  based on the piezoelectricity and the Maxwell's equations. The result is:  $E = -i(c/\nu)^2(\kappa/\zeta)u$  where  $i = (-1)^{1/2}$  is the imaginary number,





520  $v=(\mu/\rho)^{1/2}$  is the elastic wave velocity,  $\rho$  is the density ( $\text{kg/m}^3$ ) of fault-zone rocks, and  
 521  $c$  is the light speed ( $=2.999\times 10^8$  m/sec in free space),  $\zeta$  is the piezoelectric coupling  
 522 coefficient between elastic field and electric field ( $\zeta\sim 2\times 10^{-12}$  coulomb/ newton for  
 523 quartz), and  $\kappa$  is the wavenumber. Let  $L_o$  be the original length of a fault, thus leading  
 524 to  $E=-i(c/v)^2(\kappa/\zeta)(u/L_o)L_o=-i(c/v)^2(\kappa L_o/\zeta)\varepsilon$ . The three examples of geoelectric and  
 525 geomagn anomalies, thus leading to precursors of earthquakes. The precursor times of  
 526 GEM precursors should be the same as that of the pre-seismic strains. However,  
 527 Wang (2021a,b) reported different precursor times of electric field and magnetic field  
 528 even though they appeared before the same earthquake. It is necessary to explore the  
 529 reasons to cause such a difference in future.

Length of a fault, or length  
of a future earthquake  
rupture?

530 The MCD model is put into the present theory to predict the failure time and  
 531 magnitude of a forthcoming earthquake. Inserting  $E_{ij}$  and  $t_j$  ( $j=1, 2$ , and  $3$ ) into Eq. (6)  
 532 yields

$$533 \quad E_{ij}=F[a(\alpha-1)](t_f-t_j)^{(1-\alpha)} \quad (j=1, 2, 3). \quad (19)$$

536 This leads to

$$537 \quad t_f=t_j+(E_{ij}/F)^{(1-\alpha)/a}(\alpha-1) \quad (j=1, 2, 3). \quad (20)$$

540 From Eq. (20), we may predict the failure time,  $t_f$ , of the forthcoming earthquake.

541 Since  $E$  increases with  $\varepsilon$ , their precursor times are the same and thus the precursor  
 542 time,  $T$ , is  $t_f-t_o$ . Theoretically, the precursor time of the pre-seismic geoelectric  
 543 precursor is the same as that of the pre-seismic fault strains. From  $T$ , we may predict  
 544 the magnitude of the forthcoming earthquake from Eq. (18), i.e.,  $M=[\log(T)-C]/A$ .

Provide some example  
calculations to give the  
reader a sense of the values  
of these various predictions.

545 In principle, the theory works well to predict the failure time of a forthcoming  
 546 earthquake by using the pre-seismic geoelectric signals. But, in practice there might  
 547 be a problem that the values of  $E_i$  cannot be observed accurately because of the  
 548 presence of unexpected noise due to thunderstorm, atmospheric abnormal phenomena,  
 549 and artificial effects. This problem should be very serious when  $t<t_c$  because their  
 550 values are very small and cannot be observed. Hence, the observed data of geoelectric  
 551 signals must be carefully selected and corrected to remove noise. The visible  
 552 geoelectric signals should appear when  $t>t_c$  because the signals are strong enough. In

What is the basis for this  
statement? Has the author  
compared the amplitude of  
various noise sources to the  
expected signal amplitude  
of a precursor, and  
discovered that the  
precursor should be  
observable?



553 addition, in principle  $E_i$  must be measured near the fault. But, the monitoring station  
554 of geoelectric signals is usually not located near a fault where a forthcoming  
555 earthquake will happen. The value of  $E_i$  measured at a station not close to the  
556 epicenter should be slightly different from and weaker than near-fault one due to  
557 attenuation. Nevertheless, the attenuation of geoelectric signals measured at several  
558 time instants should be the same on the same station unless there are thunderstorm  
559 and abnormal atmospheric phenomena between two time instants of different stations.

560

#### 561 4.2.3 For the Geochemical Precursors

562

563 Numerous geochemical precursors are not observed at the localities near the  
564 earthquake epicenters (Wang 2021a,b; and cited references therein) because the  
565 observation stations are not installed at the sites near the epicenters. For example, Rn  
566 concentration anomalies prior to an earthquake are often observed somewhat far away  
567 from the epicenters because the measurement instruments are installed at hot-water  
568 springs or water-wells which may be far away from the epicenters. Nevertheless, their  
569 appearances are still related to the pre-seismic slip in the fault zones of forthcoming  
570 events. We assume that the presence of Rn concentration anomalies in the  
571 underground water might be associated with the spatial distribution of focal  
572 mechanism of an earthquake. The spatial pattern of the fault mechanism of an  
573 earthquake has four quarters: two for tension or dilatation and others for compression.

574 Kuo et al. (2010, 2019) reported a positive correlation between the temporal  
575 variation in Rn concentrations and that of dilatational strains measured at the Antong  
576 station for three events in southeastern Taiwan. The dilatational strains were related to  
577 tensional quarters of focal mechanisms of the events as mentioned above. They  
578 considered a model to explain Rn volatilization in an undrained fractured aquifer. This  
579 model is simply described below. A small fractured aquifer situated in a brittle rock,  
580 which is surrounded by a ductile formation in undrained conditions. When aquifer  
581 recharge is weak and negligible, undrained conditions are valid. There is only a single  
582 water phase in the aquifer before any precursory geochemical phenomenon appears.  
583 When the regional stress increases, dilation of brittle rock could occur at a faster rate  
584 than the rate of groundwater recharging into the newly created micro-cracks. As a  
585 result, gas saturation and two phases (gas and water) develop in the aquifer. The radon  
586 in groundwater volatilizes into the gas phase and the Rn concentration in groundwater

There have been several experiments in which EM or M networks have been established and maintained near to expected earthquake faults, or near an expected hypocenter. Papers based on those observations have explored the levels of noise from various sources, and evaluated whether precursory signals are observed.

Or, because there are no anomalous signals to observe.

This is the key assumption that underlies so many of these precursor studies and theories. But there is little reason to believe that regional stress should increase and accelerate ahead of an earthquake, and no observations that directly support that. If anything, stress should decrease in the vicinity of any patch of accelerating precursory slip on the fault surface.



587 decreases. The model is mathematically represented by the following equation:

588

589 
$$C_w/C_o=(HS_g+1)^{-1}$$
 (21)

590

591 where  $C_o$  is the initial Rn concentration (in pCi/L) in formation brine (salt water);  $C_w$   
592 is the equilibrium Rn concentration (in pCi/L) remaining in ground-water;  $S_g$  is the  
593 gas saturation (in %);  $H$  is Henry's coefficient (dimensionless) for Rn. From the  
594 rock-dilatancy model (Brace et al., 1966):  $\varepsilon_v=S_g/(1/\phi)$  or  $S_g=\varepsilon_v/\phi$  where  $\varepsilon_v$  and  $\phi$   
595 denote, respectively, the (dimensionless) volumetric strain of the rocks beneath the  
596 observation site and the initial fracture porosity before rock dilatancy. The volumetric  
597 strain may be represented as  $\varepsilon_1+\varepsilon_2+\varepsilon_3$  where  $\varepsilon_j$  is the strain along the  $j$ -th axis ( $j=1, 2,$   
598 and 3) (Turcotte and Schubert, 1982). This yields  $S_g=(\varepsilon_1+\varepsilon_2+\varepsilon_3)/\phi$ . Equation (19)  
599 shows that  $C_w$  increases with decreasing  $S_g$ . Inside the brittle rocks underneath the  
600 observation site,  $S_g$  increases with  $\varepsilon_v$ , thus leading to a decrease in  $C_w$ . The value of  
601  $\varepsilon_v$  inside the brittle rocks underneath the observation site will be induced by the strain  
602 in the fault zone where the forthcoming earthquake will occur. Hence, the Rn  
603 concentration changes are controlled by pre-seismic strains that occur in the related  
604 fault zone.

605 Note that although we have considered a model to describe the production of  
606 pre-seismic geochemical signals, the production processes could be more complicated  
607 than the present model. Schirripa Spagnolo et al. (2024) addressed that pre-seismic  
608 geochemical signal are produced by the transport of chemical markers throughout the  
609 aquifers producing complex spatial circulations and alterations which can be  
610 extremely difficult to grasp using just one single model. They also claimed that such  
611 complex interactions among fault zones, host rocks upper and lower crustal volumes  
612 produce a wide range feedback mechanisms. These problems are beyond the scope of  
613 this study and need further investigations.

614 Of course, the time-dependent pre-seismic slip or strain on a fault along which a  
615 forthcoming earthquake will happen can produce stress changes surrounding the fault  
616 (Aki and Richards, 1980). This might induce some geochemical precursors which  
617 occur on some places somewhat far away from the fault. Hence, such kinds of  
618 precursors will appear more or less later than the pre-seismic slip or strain that  
619 happened on the fault. This results in a shorter precursor time than that for the



pre-seismic slip or strain. Here, we consider a mechanical model to explain the problem. Dobrovolsky et al. (1979) used a half space, during the preparation processes of an earthquake, a zone of cracked rocks is formed in the focal area under the tectonic loading,  $\tau$ . The media inside the zone may be considered as a solid inclusion with different moduli that are lower than that of the half space. The solid inclusion re-distributes the stresses accompanied by deformations, including those on the Earth's ground surface. Let  $V$  be the solid soft inclusion volume that is an ellipse with a long-axis length of  $l_l$  and a short-axis length of  $l_s$ :  $l_l > l_s$  for  $M \geq 5$  and  $l_l = l_s$  for  $M < 5$ , thus leading to  $V = \pi l_l l_s^2 / 6$  for  $M \geq 5$  and  $V = \pi l_s^3 / 6$  for  $M < 5$ . The shear modulus of the half space and that of the inclusion are  $\mu$  and  $\mu - \delta\mu$ , respectively. The ratio  $\delta\mu/\mu$  is denoted by  $\varphi$ . Assuming that the zone of effective manifestation of the precursory deformations is a sphere with the center at the epicenter of the forthcoming earthquake under the shear stresses loaded at infinity. In the spherical zone with a radius of  $r_\varepsilon$ , the deformation has a strain being equal to or exceeding a certain  $\varepsilon_s$  which is smaller than the strain on the related fault. The  $r_\varepsilon$  is called the 'strain radius.' They obtained  $r_\varepsilon = 0.85(\varphi V \tau / \mu \varepsilon_s)^{1/3}$ . This leads to

$$\varepsilon_s = (0.85)^3 \varphi V \tau / \mu r_\varepsilon^3. \quad (22)$$

This reveals that the strain decreases when the radius or the distance from the earthquake hypocenter increases. Based on Eq. (22), Rn concentration anomaly could occur at a distance  $r_\varepsilon$  from the hypocenter when the strain at the observation site is larger than  $\varepsilon_s$ . Hence, the pre-seismic strain in the related fault zone must be larger than a particular value,  $\varepsilon_p$  ( $> \varepsilon_s$ ), at time  $t = t_p$ . This makes the occurrence time of Rn concentration anomaly be later than that of the pre-seismic strain because of  $t_p > t_o$ . Thus, the precursor time of the former is shorter than that of the latter. Equation (5) becomes

$$\varepsilon(t) - \varepsilon_p = \{ [a(\alpha-1)(t_f - t_p) + \varepsilon_{ff}^{1-\alpha}]^\eta - [a(\alpha-1)(t_f - t) + \varepsilon_{ff}^{1-\alpha}]^\eta \} / a(\alpha-2). \quad (23)$$

Define  $T = t_f - t_p$  to be the precursor time of this precursor. Considering  $\varepsilon_p = \gamma \varepsilon_{ff}$  and  $\varepsilon_{ff} \gg 1$ , Eq. (23) hence becomes

In most of the paper, the assumption is that there is precursory strain related to the entire future fault area, not specifically the hypocenter or epicenter. The author should point this out, and explain why it is reasonable to consider these two contrasting views of precursory processes.

If I follow correctly, this is a comparison between strain changes that scale with  $M_s$ , to Rn anomalies that are focussed around the hypocenter. Why is it not the case that e-sub-f is also concentrated at the future hypocenter?



$$(1-\gamma)\varepsilon_f = \{[a(\alpha-1)T]^\eta/a(\alpha-2)\}. \quad (24)$$

654

655 This yields

656

$$T = [a(\alpha-2)(1-\gamma)\varepsilon_f]^{1/\eta/a(\alpha-1)}. \quad (25)$$

658

659 Taking the logarithm on the two sides of Eq. (25) leads to

660

$$\log(T) = [a(\alpha-2)(1-\gamma)\varepsilon_f]^{1/\eta/a(\alpha-1)}. \quad (26)$$

662

663 This gives

664

$$\log(T) = C' + AM_w \quad (27)$$

666

667 where  $C' = (1-\gamma)C < C$ . This indicates that when the Rn concentration anomaly is taken  
 668 as a precursor, only the value of the constant is reduced from  $C$  to  $C'$ , while the  
 669 scaling exponent  $A$  does not change because of the same fault zone. This again to  
 670 confirm the importance of the  $\log(T)$ – $M$  relationship on the assessment of a  
 671 forthcoming earthquake. When two groups of earthquakes occur in two fault systems  
 672 whose rock materials have different values of  $a$  and  $\alpha$ , their values of  $C$  and  $A$  could  
 673 be different, thus resulting in different  $\log(T)$ – $M$  relationships.

674 For Rn concentration anomalies before six earthquakes with  $M=5.0$ – $6.8$  and  
 675  $d=7.0$ – $35.6$  km ( $M$ =the local magnitude;  $d$ =the focal depth, in km) in southeastern  
 676 Taiwan, Kuo et al. (2020) obtained  $\log(T)=1.456+0.053M$ . For the Rn concentration  
 677 anomalies before 9 events in northern Taiwan, Wang (2023) obtained  $\log(T)=$   
 678  $(-0.21\pm0.30)+(0.23\pm0.02)M$ . For the Rn concentration anomalies before 111  
 679 earthquakes in Taiwan, Wang (2021b) obtained  $\log(T)=(-2.05\pm0.40)+(0.58\pm0.01)M$   
 680 for the events with  $d\leq 40$  km and  $\Delta\leq 40$  km ( $\Delta$ =the focal depth, in km); and  $\log(T)=$   
 681  $(-0.40\pm0.42)+(0.26\pm0.01)M$  for those with  $d>40$  km or  $\Delta>40$  km. The  $\log(T)$ – $M$   
 682 relationship for northern Taiwan is different from that for southeastern Taiwan. This  
 683 indicates the difference on  $a$  of the fault-zone rocks between the two areas. The  
 684  $\log(T)$ – $M$  relationship for northern Taiwan is different from those for Taiwan in two  
 685 different focal-depth ranges. This suggests that there is a difference on  $\alpha$  of the

Again, provide a table that calculates T for various values of M.

What are the units of T?



686 fault-zone rocks between northern Taiwan and the whole Taiwan region. That the  
687  $\log(T)$ – $M$  relationships for Taiwan in two different focal-depth ranges suggests that  
688 the fault-zone rocks in the two different focal-depth ranges are different from each  
689 other.

690 We assume that the theory proposed in this study can be applied to other kinds of  
691 precursors, and thus the  $\log(T)$ – $M$  relationships exist for these precursors as  
692 mentioned above. Based on the difference of the  $\log(T)$ – $M$  relationships between two  
693 kinds of precursors, Wang (2023) suggested a method to predict the failure time and  
694 magnitude of a forthcoming earthquake directly from observations. He explored in  
695 details the conditions of the values of  $C'$  and  $A$  of Eq. (25) for two different  
696 precursors that can be used for earthquake prediction. He also gave examples for  
697 geochemical precursors to show how to predict the failure time and magnitude of a  
698 forthcoming mainshock. The present theory provides the physical basis of his study.

699

## 700 5. Conclusions

701

702 From the subcritical crack growth model, we propose a theory of predicting a  
703 forthcoming earthquake from pre-seismic strain signals. We consider three aspects:  
704 prediction of failure time, prediction of earthquake magnitude, and prediction of  
705 location. The pre-seismic strain is here considered as a fundamental and important  
706 earthquake precursor. Based on the Voight's equation for failure of materials under  
707 stresses, we theoretically investigate the physical basis on predicting the failure time  
708 and magnitude of a forthcoming earthquake in terms of pre-seismic anomalous strain  
709 signals which are generated on or near the fault where the event will happen.  
710 Meanwhile, the present study demonstrates the physical basis of the  $\log(T)$ – $M$   
711 relationships of precursors. Results exhibit that the failure time depends on the strain  
712 rate and two parameters of the Voight's equation; while the magnitude are controlled  
713 by the precursor time, two parameters of the Voight's equation, and the exponent of  
714 the scaling law between the co-seismic strain and the fault length. The scaling  
715 exponent,  $\alpha$ , of the Voight's equation is an important factor on the  $\log(T)$ – $M$   
716 relationship. Although the location of a forthcoming earthquake cannot be determined  
717 from the present theory, it may still be qualitatively assessed from the observations.  
718 The theory may be applied to the  $\log(T)$ – $M$  relationships of other kinds of precursors.

A lot of information has been presented in this paper. It would be helpful to add a short discussion section in which examples are given for how a scientist might practically proceed: Given an observational network (e.g., of strain, or  $R_n$ , or something else), what steps are required to obtain useful estimates of the future earthquake's time and magnitude?



719 Based on the theoretical results made by Main (1998) and the observed values of  $A$  of  
720 the relationships, the value of  $\alpha$  must be in the range 1.0 to 1.8 for the generation of  
721 earthquakes. The  $\log(T)$ – $M$  relationships of pre-seismic geoelectromagnetic and  
722 geochemical signals are taken into account. Theoretical results reveal that the  
723 precursor times of the pre-seismic geoelectromagnetic precursors and those of  
724 geochemical precursors are, respectively, the same and shorter than that of the  
725 pre-seismic strains.

726

727 *Data availability.* No

728

729 *Competing interests.* There are no known competing financial interests or personal  
730 relationships that could have appeared to influence the work reported in this paper.

731

732 *Acknowledgments.* This study was supported by the Institute of Earth Sciences,  
733 Academia Sinica, Taiwan, ROC.

734

## 735 **References**

736

737 Aki, K.: Ideal probabilistic earthquake prediction, *Tectonophys.*, 169, 197-198,  
738 DOI:10.1016/0040-1951(89)90193-5, 1989.

739 Aki, K.: *Seismology of Earthquake and Volcano Prediction*. Science Press Beijing,  
740 China, 331 pp (with Chinese translation), 2009.

741 Aki, K. and Richard, P.G.: *Quantitative Seismology*. H. Freeman and Co., San  
742 Francisco, 932pp, 1980.

743 Atkinson, R.K.: Subcritical crack growth in geological materials, *J. Geophys. Res.*, 89,  
744 4077-4114, 1984.

745 Atkinson, B.K.: Introduction to fracture mechanics and its geophysical applications,  
746 In: Atkinson, B.K. (Ed.), *Fracture Mechanics of Rock*, 1-26, Academic Press,  
747 London, 1987.

748 Atkinson, B.K. and Meredith, P.G.: Experimental fracture mechanics data for rocks  
749 and minerals, In: Atkinson, B.K. (Ed.), *Fracture Mechanics of Rock*, Academic  
750 Press. London, 477-525 1987.

751 Bak, P.: *How nature works: the science of self-organized criticality*. Springer

Again, it's been 27 years since Main (1998). Has there been any work or observations that may be used to estimate alpha for seismogenic crust?



- 752 Science+Business Media, LLC, 212 pp, 1996.
- 753 Bernard, P.: Plausibility of long distance electrotelluric precursors of earthquakes, J.  
754 Geophys. Res., 97, 17531-17546, 1992.
- 755 Bishop, J.R.: Piezoelectric effects in quartz-rich rocks, Tectonophys., 77, 297-321,  
756 1981.
- 757 Bowman, D.D., Ouillon, G., Sammis, C.G., Sornette, A., and Sornette, D.: An  
758 observational test of the critical earthquake concept, J. Geophys. Res., 103,  
759 24359- 24372, 1998.
- 760 Brace, W.F., Paulding, B.W. Jr., and Scholz, C.H.: Dilatancy in the fracture of  
761 crystalline rocks, J. Geophys. Res., 71, 3939-3953, doi:10.1029/J  
762 Z071i016p03939, 1966.
- 763 Bufo, C.G. and Vannres, D.J.: Predicting modeling of the seismic cycle of the greater  
764 San Francisco Bay region, J. Geophys. Res., 98, 9871-9883, 1993.
- 765 Cornelius, R.R. and Voight, B.: Graphical and PC-software analysis of volcano  
766 eruption precursors according to the Materials Failure Forecast Method (FFM), J  
767 Volcanol. Geotherm. Res., 64, 295-320, 1995.
- 768 Chen, K.C. and Wang, J.H.: On the studies of the May 10, 1983 Taipingshan, Taiwan  
769 earthquake sequence, Bull. Inst. Earth Sci., Acad. Sin., ROC, 4, 1-27, 1984.
- 770 Chen, K.C., Wang, J.H., and Yeh, Y.L.: Premonitory phenomena of a moderate  
771 Taiwan earthquake, Terr. Atmos. Ocean. Sci., 1, 1-21, 1990.
- 772 Cianchini, G., De Santis, A., Di Giovambattista, R., Abbattista, C., Amoroso, L.,  
773 Campuzano, S.A., Carbone, M., Cesaroni, C., De Santis, A., Marchetti, D.,  
774 Perrone, L., Piscini, A., Santoro, F., and Spogli, L.: Revised accelerated moment  
775 release under test: fourteen worldwide real case studies in 2014–2018 and  
776 simulations, Pure Appl. Geophys., 177, 4057- 4087, 2020.
- 777 Corson, D. and Lorrain, P.: Introduction to Electromagnetic Field and Waves,  
778 Freeman, San Francisco, 552 pp, 1962.
- 779 Das, S. and Scholz, C.H.: Theory of time-dependent rupture in the earth, J. Geophys.  
780 Res., 86, 6039-6051, 1981.
- 781 De Santis, A., Cianchini, G., and Di Giovambattista, R.: Accelerating moment release  
782 revisited: Examples of application to Italian seismic sequences, Tectonophys.,  
783 639, 82-98, 2015.
- 784 De Santis, A., Marchetti, D., Spogli, L., Cianchini, G., Pavón-Carrasco, F.J.,  
785 Franceschi, G.D., Di Giovambattista, R., Perrone, L., Qamili, E., Cesaroni, C.,





- 786 De Santis, A., Ippolito, A., Piscini, A., Campuzano, S.A., Sabbagh, D., Amoroso,  
787 L., Carbone, M., Santoro, F., Abbattista, C., and Drimaco, D.: Magnetic field and  
788 electron density data analysis from swarm satellites searching for ionospheric  
789 effects by great earthquakes: 12 case studies from 2014 to 2016, *Atmosphere*,  
790 10(7), 371, 2019.
- 791 Dieterich, J.H.: Preseismic fault slip and earthquake prediction, *J. Geophys. Res.*,  
792 83(B8), 3940-3948, 1978.
- 793 Ding, G.y., Ma, T.c., and Ma, S.j.: Methods of earthquake prediction, In: *Earthquake*  
794 *Prediction*, Evison, F.F. (Ed.), Terra Scientific Publishing Co., Tokyo, Unesco,  
795 Paris, 453-465, 1985.
- 796 Dobrovolsky, I.P., Zubkov, S.I., and Miachkin, V.I.: Estimation of the size of  
797 earthquake preparation zone, *Pure Appl. Geophys.*, 117, 1025-1044, 1979.
- 798 Enomoto, Y.: Coupled interaction of earthquake nucleation with deep Earth gases: a  
799 possible mechanism for seismo-electromagnetic phenomena, *Geophys. J. Intl.*,  
800 191, 1210-1214, 2012.
- 801 Freund, F.: Charge generation and propagation in igneous rocks, *J. Geodyn.*, 33,  
802 543-570. doi:10.1016/S0264-3707(02)00015-7, 2002.
- 803 Fu, C.C., and Lee, L.C.: Continuous monitoring of fluid and gas geochemistry for  
804 seismic study in Taiwan, In: *Pre-Earthquake Processes: A Multidisciplinary*  
805 *Approach to Earthquake Prediction Studies*, Ouzounov, D., Pulinets, S., Hattori,  
806 K., and Taylor, P. (Eds.), *Geophysical Monograph Series*, 234, 199-218, 2018.
- 807 Fujinawa, Y., Noda, Y., Takahashi, K., Kobayashi, M., Takamatsu, K., and  
808 Natsumeda, J.: Field detection of microcracks to define the nucleation stage of  
809 earthquake occurrence, *Intern. J. Geophys.*, 2013, 1-18, Article ID  
810 651823, <http://dx.doi.org/10.1155/2013/651823>, 2002.
- 811 Geller, R.J.: Earthquake prediction: a critical review, *Geophys. J. Int.*, 131, 425-450,  
812 1997.
- 813 Geller, R.J., Jackson, D.D., Kagan, Y.Y., and Mulargia, F.: Earthquakes cannot be  
814 predicted, *Science*, 275, 1616-1617, doi:10.1126/science.275.5306.1616, 1997.
- 815 Gutenberg B. and Richter, C.F.: Earthquake magnitude, intensity, energy and  
816 acceleration, *Bull. Seism. Soc. Am.*, 32, 163-191, 1942.
- 817 Gutenberg, B. and Richter, C.F.: Frequency of earthquakes in California, *Bull. Seism.*  
818 *Soc. Am.*, 34, 185-188, 1944.
- 819 Gulia, L. and Wiemer, S.: Real-time discrimination of earthquake foreshocks and



- 820 aftershocks, *Nature*, 574(7777), 193-199, 2019.
- 821 Gutenberg, B. and Richter, C.F.: Magnitude and energy of earthquake, *Annali de*  
822 *Geofisica*, 9, 1-15, 1956.
- 823 Hayakawa, M. and Hobara, Y.: Current status of seismo-electromagnetic for  
824 short-term earthquake prediction, *Geomatics Natural Hazards Risk*, 1(2),  
825 115-155, 2010.
- 826 Hayakawa, M., Ohta, K., Maekawa, S., Yamauchi, T., Ida, Y., Gotoh, T., Yonaiguchi,  
827 N., Sasaki, H., and Nakamura T.: Electromagnetic precursors to the 2004 Mid  
828 Niigata Prefecture earthquake, *Phys. Chem. Earth*, 31, 356-364, 2006.
- 829 Kanamori, H.: Mode of strain release associated with major earthquake in Japan, *Ann.*  
830 *Rev. Earth Planet. Sci.*, 1, 213-239, 1973.
- 831 Kanamori, H.: Initiation process of earthquakes and its implications for seismic  
832 hazard reduction strategy, *Proc. Natl. Acad. Sci. USA*, 93, 3830-3837, 1996.
- 833 Kanamori, H. and Anderson, D.L.: Theoretical basis of some empirical relations in  
834 seismology, *Bull. Seism. Soc. Am.*, 65, 1073-1095, 1975.
- 835 Kanamori, H. and Heaton, T.H.: Microscopic and macroscopic physics of earthquakes,  
836 In: Rundle, J.B., Turcotte, D.L., and Klein, W. (Eds.), *Geocomplexity and*  
837 *Physics of Earthquakes*, *Am. Geophys. Monog.*, 120, 147-163, 2000.
- 838 Kilburn, C.R. and Voight, B.: Slow rock fracture as eruption precursor at Soufriere  
839 Hills volcano, Montserrat, *Geophys. Res. Letts.*, 29, 3665-3668, 1998.
- 840 Knopoff, L.: Energy release in earthquakes, *Geophys. J.*, 1, 44-52, 1958.
- 841 Knopoff, L.: Earthquake prediction: The scientific challenge, *Proc. Nat. Acad. Sci.*,  
842 *USA*, 93, 3719-3720 (1996)
- 843 Kostrov, B.V., Das, S.: Idealized models of fault behavior prior to dynamic rupture.  
844 *Bull. Seism. Soc. Am.*, 72, 679-703, 1982.
- 845 Kuhn, T.S.: *The Structure of Scientific Revolutions*. The University of Chicago Press,  
846 *USA*, 210 pp, 1962.
- 847 Kuo, C.L., Lee, L.C., and Huba, J.D.: An improved coupling model for the  
848 lithosphere-atmosphere-ionosphere system, *J. Geophys. Res.: Space Phys.*, 119,  
849 3189-3205, doi:10.1002/2013JA019392, 2014.
- 850 Kuo, C.L., Huba, J.D., Joyce, G., and Lee, L.C.: Ionosphere plasma bubbles and  
851 density variations induced by pre-earthquake rock currents and associated  
852 surface charges, *J. Geophys. Res.*, 116, A10317, doi:10.1029/2011ja016628,  
853 2011.



- 854 Kuo, T., Chen, W., Ho, C., and Kuochen, H., Chiang, C.: In-situ radon volatilization  
855 in an undrained fractured aquifer, Proc., 44th Workshop Geothermal Reservoir  
856 Engineer., 11-13, Stanford Univ., Stanford, Cal., USA, Feb., 2019.
- 857 Kuo, T., Lin, C., Chang, G., Fan, K., and Cheng, W., Lewis, C.: Estimation of  
858 aseismic crustal strain using radon precursors of the 2003 M6.8, 2006 M6.1, and  
859 2008 M5.0 earthquakes in eastern Taiwan, Nat. Hazards, 53, 219-228, 2010.
- 860 Kuo, T., Chen, W., Ho, C., Kuochen, H., and Chiang, C.: Precursory behavior of  
861 groundwater radon in Southeastern Taiwan: Effect of tectonic setting in the  
862 subduction zone, Pure Appl. Geophys., 177, 2877-2887, <https://doi.org/10.1007/s00024-019-02389-9>, 2020.
- 863
- 864 Leonard, M.: Earthquake fault scaling: Self-consistent relating of rupture length,  
865 width, average displacement, and moment release, Bull. Seism. Soc. Am.,  
866 100(5A), 1971-1988, 2010.
- 867 Lomnitz, C. and Lomnitz-Adler, J.: A framework for earthquake prediction, In:  
868 Earthquake Prediction: An International Review, 575-578, 1981.
- 869 Madden, T.R. and Mackie, R.L.: What electric measurements can say about changes  
870 in fault systems, Proc. Natl. Acad. Sci., USA, 93, 3776-3780, 1996.
- 871 Main, I.G.: Prediction of failure times in the earth for a time-varying stress, Geophys.  
872 J., 92, 455-464, 1988.
- 873 Main, I.G.: Applicability of time-to-failure analysis to accelerated strain before  
874 earthquakes and volcanic eruptions, Geophys. J. Int., 139, F1-F6, 1999.
- 875 Main, I.G. and Meredith, P.G.: Classification of earthquake precursors from a fracture  
876 mechanics model, Tectonophysics., 167, 273-283, 1989.
- 877 Martin, R.J.: Is piezomagnetism influenced by microcracks during cyclic loading?, J.  
878 Geomag. Geoelectr., 32, 741-756, 1980.
- 879 Meredith, P.G. and Atkinson, B.K.: Stress corrosion and acoustic emission during  
880 tensile crack propagation in Whin Sill dolerite and other basic rocks, Geophys.  
881 J.R. Astron. Soc., 75, 1-21, 1983.
- 882 Milne, J.: Seismic science in Japan, Trans. Seism. Soc. Jpn., 1, 3-33, 1880.
- 883 Mizutani, H., Ishida, T., Yokokura, T., and Ohnishi, S.: Electrokinetic phenomena  
884 associated with earthquakes, Geophys. Res. Lett., 3, 365-368, 1976.
- 885 Molchanov, O.A. and Hayakawa, M.: Generation of ULF electromagnetic emission  
886 by microfracturing, Geophys. Res. Letts., 22(22), 3091-3094, 1995.
- 887 Namgaladze, A.A., Zolotov, O.V., Karpov, M.I., and Romanovskaya, Y.V.:



- 888 Manifestations of the earthquake preparations in the ionosphere total electron  
889 content variations, *Nat. Sci.*, 4(11), 848-855, doi:10.4236/ns.2012.411113, 2012.
- 890 Ogawa, T., Oike, K., and Miura, T.: Electromagnetic radiation from rocks, *J. Geophys.*  
891 *Res.*, 90, 6245-6249, 1985.
- 892 Ohta, K., Watanabe, N., and Hayakawa, M.: The observation of ULF emissions at  
893 Nakatsugawa in possible association with the 2004 Mid Niigata Prefecture  
894 earthquake, *Earth Planets Space*, 57, 1003-1008, 2005.
- 895 Ouzounov, D., Pulinets, S., Hattori, K., and Taylor, P. (Eds.): *Pre-Earthquake*  
896 *Processes: A Multidisciplinary Approach to Earthquake Prediction Studies*. AGU  
897 publication, 384 pp, 2018.
- 898 Papazachos, C.B., Karakaisis, G.F., Savvaidis, A.S., and Papazachos, B.C.:  
899 Accelerating seismic crustal deformation in the Southern Aegean area, *Bull.*  
900 *Seism. Soc. Am.*, 92(2), 570-580, 2002.
- 901 Potirakis, S.M., Hayakawa, M., and Schekotov, A.: Fractal analysis of the  
902 ground-recorded ULF magnetic fields prior to the 11 March 2011 Tohoku  
903 earthquake ( $M_w=9$ ): discriminating possible earthquake precursors from space-  
904 sourced disturbances, *Nat. Hazards*, 85, 59-86, [https://doi.org/10.1007/s11069-](https://doi.org/10.1007/s11069-016-2558-8)  
905 [016-2558-8](https://doi.org/10.1007/s11069-016-2558-8), 2017.
- 906 Pulinets, S. and Ouzounov, M.D.: Lithosphere–Atmosphere–Ionosphere Coupling  
907 (LAIC) model – An unified concept for earthquake precursors validation, *J.*  
908 *Asian Earth Sci.*, 41, 371-382, 2011.
- 909 Pulinets, S., Ouzounov, D., Karelin, A., and Davidenko, D.: Lithosphere–  
910 Atmosphere–Ionosphere–Magnetosphere Coupling – A Concept for Pre-  
911 earthquake Signals Generation, In: Ouzounov, D., Pulinets, S., Hattori, K., and  
912 Taylor, P. (Eds.), *Pre-Earthquake Processes: A Multidisciplinary Approach to*  
913 *Earthquake Prediction Studies*, *Geophys. Monog. Series*, 234, 79-98, 2018.
- 914 Reid, H.F.: The mechanics of the earthquake, *Rept. State Earthquake Inv. Comm.*, The  
915 California Earthquake of April 18, 1906, Washington, D.C., Carnegie Inst., 1910.
- 916 Rikitake, T.: Dilatancy model and empirical formulas for an earthquake area, *Pure*  
917 *Appl. Geophys.*, 113, 141-147, 1975a.
- 918 Rikitake, T.: Earthquake precursors, *Bull. Seism. Soc. Am.*, 65, 1133-1162, 1975b.
- 919 Rikitake, T.: Classification of earthquake precursors, *Tectonophys.*, 54, 293-308,  
920 1979.
- 921 Rikitake, T.: Earthquake precursors, In: Evison, F.F. (Ed.), *Earthquake Prediction*,



- 922 Terra Scientific Publishing Co., Tokyo, Unesco, Paris, 3-21, 1984.
- 923 Rikitake, T. and Yamazaki, Y.: The nature of resistivity precursor, Earthquake Pred.  
924 Res., 3, 559-570, 1985.
- 925 Rudnicki, J.W.: Physical models of earthquake instability and precursory processes,  
926 Pure Appl. Geophys., 126(2-4), 531-554, 1988.
- 927 Rundle, J.B., Klein, W., Turcotte D.L., and Malamud, B.D.: Precursory seismic  
928 activation and critical-point phenomena, Pure Appl. Geophys., 157, 2165-2182,  
929 doi:10.1007/PL00001079, 2000.
- 930 Sarkar, I.: Possible precursory accelerated Benioff strain in the region of Sistan Suture  
931 Zone of Eastern Iran, Acta Geophysica, 59(2), 239-261, 2011.
- 932 Sasai, Y.: The piezomagnetic field associated with the Mogi model, Bull. Earthq. Res.  
933 Inst., Tokyo Univ., 54, 1-29, 1979.
- 934 Sasai, Y.: Application of the elasticity theory of dislocations to tectonomagnetic  
935 modeling, Bull. Earthq. Res. Inst., Univ. Tokyo, 55, 387-447, (in Japanese with  
936 English abstract), 1980.
- 937 Savage, B., Komatitsch, D., and Tromp J.: Effects of 3D attenuation on seismic wave  
938 amplitude and phase measurements, Bull. Seism. Soc. Am., 100(3), 1241-1251,  
939 doi:10.1785/0120090263, 2010.
- 940 Schirripa Spagnolo, G., Bernasconi, S.M., Aldega, L., Castorina,  
941 F., Billi, A., Smeraglia, L., Agosta, F., Prosser, G., Tavani, S., and Carminati,  
942 E.: Interplay and feedback between tectonic regime, faulting, sealing horizons,  
943 and fluid flow in a hydrocarbon-hosting extensional basin: The Val d'Agri Basin  
944 case, Southern Italy, Earth Planet. Sci. Letts., 646,  
945 118982, <https://doi.org/10.1016/j.epsl.2024.118982>, 2024.
- 946 Scholz, C.H.: The Mechanics of Earthquakes and Faulting. Cambridge Univ. Press,  
947 Cambridge, UK, 439 pp, 1990.
- 948 Scholz, C.H., Sykes, L.R., and Aggarwal, Y.P.: Earthquake prediction: A physical  
949 basis. Science, 181, 803-810, doi:10.1126/science.181.4102.803, 1973.
- 950 **Shaw, C.H.**: Magnitude and slip scaling relations for fault-based seismic hazard. Bull.  
951 Seism Soc. Am., 113(3), 924-947, <https://doi.org/10.1785/0120220144>, 2023.
- 952 Sibson, R.H.: Fault rocks and fault mechanisms, J. Geol. Soc. Landon. 133, 191-213,  
953 1977.
- 954 Slifkin, L.: Seismic electric signals from displacement of charged dislocations,  
955 Tectonophys., 224, 149-152, 1993.

The author's name is  
Bruce E. Shaw (B.E.  
Shaw).



- 956 Smith, W.D.: The b-value as an earthquake precursor. *Nature*, 289, 136-139,  
957 doi:10.1038/289136a0, 1981.
- 958 Smith, W.D.: Evidence for precursory changes in the frequency-magnitude b-value,  
959 *Geophys. J. R. astro. Soc.*, 86, 815-838, 1986.
- 960 Sornette, D.. Mechanochemistry: An hypothesis for shallow earthquakes,  
961 In: Teisseyre, R. and Majewski, E. (Eds.), *Earthquake Thermodynamics and*  
962 *Phase Transformation in the Earth's Interior*, 1<sup>st</sup> Edition, Cambridge Univ. Press,  
963 Cambridge, UK, 674 pp, 2001.
- 964 Stauffer, D. and Aharony, A.: *Introduction to Percolation Theory*. Taylor and Francis,  
965 London, 1994.
- 966 Thingbaijam, K.K.S., Mai, P.M., and Goda, K.: New empirical earthquake  
967 source-scaling laws, *Bull. Seism. Soc. Am.*, 107(5), 2225-2246, 2017.
- 968 Tsubokawa, I.: On relation between duration of crustal movement and magnitude of  
969 earthquake expected, *J. Geod. Soc. Japan*, 15, 75-88, (in Japanese), 1969.
- 970 Tsubokawa, I.: On relation between duration of precursory phenomena and duration  
971 of crustal movement and magnitude before earthquake, *J. Geod. Soc. Japan*, 19,  
972 116-119, (in Japanese), 1973.
- 973 Tsubokawa, I., Ogawa, Y., and Hayashi, T.: Crustal movement before and after the  
974 Niigata earthquake, *J. Geod. Soc. Japan*, 10, 165-171, 1964.
- 975 Turcotte, D.L. and Schubert, G.: *GEODYNAMICS – Applications of Continuum*  
976 *Physics to Geological Problems*. Wiley, 450 pp, 1982.
- 977 Turcotte, D.L., Newman, W.L., and Shcherbakov, R.. Micro and macroscopic models  
978 of rock fracture, *Geophys. J. Int.*, 152, 718-728, 2003
- 979 Tzanis, A. and Vallianatos, F.: A physical model of electrical earthquake precursors  
980 due to crack propagation and the motion of charged edge dislocations, In:  
981 *Seismo Electromagnetics (Lithosphere–Atmosphere–Ionosphere–Coupling)*,  
982 TerraPub, 117-130, 2002.
- 983 Vallianatos, F. and Tzanis, A.: Electric current generation associated with the  
984 deformation rate of a solid: Preseismic and coseismic signals, *Phys. Chem. Earth*,  
985 23, 933-938, 1998.
- 986 van Deelen, G.: U.S. earthquake early warning system gets a major upgrade, *Eos*,  
987 105, <https://doi.org/10.1029/2024EO240363>, 2024.
- 988 Varnes, D.J.: Predicting earthquake by analyzing accelerating precursory seismic  
989 activity, *Pure Appl. Geophys.*, 130, 661-686, 1989.



- 990 Venegas-Aravena, P., Cordaro, E.G., and Laroze, D.: A review and upgrade of the  
991 lithospheric dynamics in context of the seismo-electromagnetic theory, *Nat.*  
992 *Hazards Earth Syst. Sci.*, 19,  
993 1639-1651, <https://doi.org/10.5194/nhess-19-1639-2019>, 2019
- 994 Voight, B.: A method for prediction of volcanic eruptions, *Nature*, 332, 125-130,  
995 1988.
- 996 Voight, B.: A relation to describe rate-dependent material failure, *Science*, 243, 200-  
997 203, 1989.
- 998 Wang, J.H.: The seismic efficiency of the 1999 Chi-Chi, Taiwan, earthquake, *Geophys.*  
999 *Res. Letts.*, 31, L10613, doi:10.1029/204GL019417, 2004,
- 1000 Wang, J.H.: Effect of thermal pressurization on the radiation efficiency, *Bull. Seism.*  
1001 *Soc. Am.*, 99(4), 2293-2304, 2009.
- 1002 Wang, J.H.: A review on scaling of earthquake faults, *Terr. Atmos. Ocean. Sci.*, 29(6),  
1003 589-610, 2018.
- 1004 Wang, J.H.: A review on precursors of the 1999  $M_w$ 7.6 Chi-Chi, Taiwan, earthquake,  
1005 *Terr. Atmos. Ocean. Sci.*, 32(3), 275-304, doi:10.3319/TAO.2021.03.24.01,  
1006 2021a.
- 1007 Wang, J.H.: A compilation of precursor times of earthquakes in Taiwan, *Terr. Atmos.*  
1008 *Ocean. Sci.*, 32(4), 411-441, doi:10.3319/TAO.2021.07.12.01, 2021b.
- 1009 Wang, J.H.: Piezoelectricity as a mechanism on generation of electromagnetic  
1010 precursors before earthquakes, *Geophys. J. Int.*, 224, 682-700, 2021c.
- 1011 Wang, J.H.: A physical basis of predicting the magnitude and failure time of a  
1012 forthcoming earthquake, *Ann. Geophys.*, 66, 6, doi:10.4401/ag-8914, 2023,
- 1013 Wang, J.H., Chen, K.C., Leu, P.L., and Chang, C.H.: Precursor times of abnormal  
1014 b-values prior to earthquakes, *J. Seismol.*, 20(3), 905-919, DOI:10.1007/s10950-  
1015 016-9567-7, 2016.
- 1016 Wang, K., Chen, Q.F., Sun, S., and Wang, A.: Predicting the 1975 Haicheng  
1017 earthquake. *Bull. Seism. Soc. Am.*, 96, 757-795, doi:10.1785/0120050191, 2006.
- 1018 Wells, D.L. and Coppersmith, K.J.: New empirical relationships among magnitude,  
1019 rupture length, rupture width, rupture area, and surface displacement, *Bull.*  
1020 *Seism. Soc. Am.*, 84(4), 974-1002, 1994.
- 1021 Whitcomb, J.H., Garmany, J.D., and Anderson, D.L.: Earthquake prediction:  
1022 Variation of seismic velocities before the San Fernando earthquake, *Science*, 180,  
1023 632, 1973.



- 1024 Whitworth, R.W.: Charged dislocations in ionic crystals, *Adv. Phys.*, 24, 203-304,  
1025 1975.
- 1026 Wu, Y.H., Chen, C.c., Rundle, J.B., and Wang, J.H.: Regional dependence of seismic  
1027 migration pattern, *Terr. Atmos. Ocean. Sci.*, 23(2), 161-170, 2012.
- 1028 Wyss, M., Aceves, R.L., and Park S.K.: Cannot earthquakes be predicted?, *Science*,  
1029 278, 487-490, 1997.
- 1030 Yu, S.B., Kuo, L.C., Hsu, Y.J., Su, H.H., Liu, C.C., Hou, C.S., Lee, J.F., Lai, T.C.,  
1031 Liu, C.C., Liu, C.L., Tseng, T.F., Tsai, C.S., and Shin, T.C.: Preseismic  
1032 deformation and coseismic displacements associated with the 1999 Chi-Chi,  
1033 Taiwan, earthquake. *Bull. Seism. Soc. Am.*, 91, 995-1012, 2001.
- 1034 Zaccagnino, D. and Doglioni, C.: The impact of faulting complexity and type on  
1035 earthquake rupture dynamics. *Communications Earth & Environment*, 3,  
1036 358, <https://doi.org/10.1038/s43247-022-00593-5>, 2022
- 1037 Zaccagnino, D., Vallianatos, F., Michas, G., Telesca, L., and Doglioni, C.: Are  
1038 foreshocks fore-shocks?, *J. Geophys. Res.: Solid Earth*, 129(2), e2023JB027337,  
1039 2024.
- 1040 Zolotov, O.V., Prokhorov, B.E., Namgaladze, A.A., and Martynenko, G.V.:  
1041 Variations in the total electron content of the ionosphere during preparation of  
1042 earthquakes, *Russ. J. Phys. Chem. B*, 5(3), 435-438, doi:10.1134/  
1043 s1990793111030146, 2011.
- 1044 Zolotov, O.V., Namgaladze, A.A., Zakharenkova, I.E., Martynenko, O.V., and  
1045 Shagimuratov, I.I.: Physical interpretation and mathematical simulation of  
1046 ionospheric precursors of earthquakes at midlatitudes, *Geomagn. Aeron.*, 52(3),  
1047 390-397, doi:10.1134/S0016793212030152, 2012.
- 1048



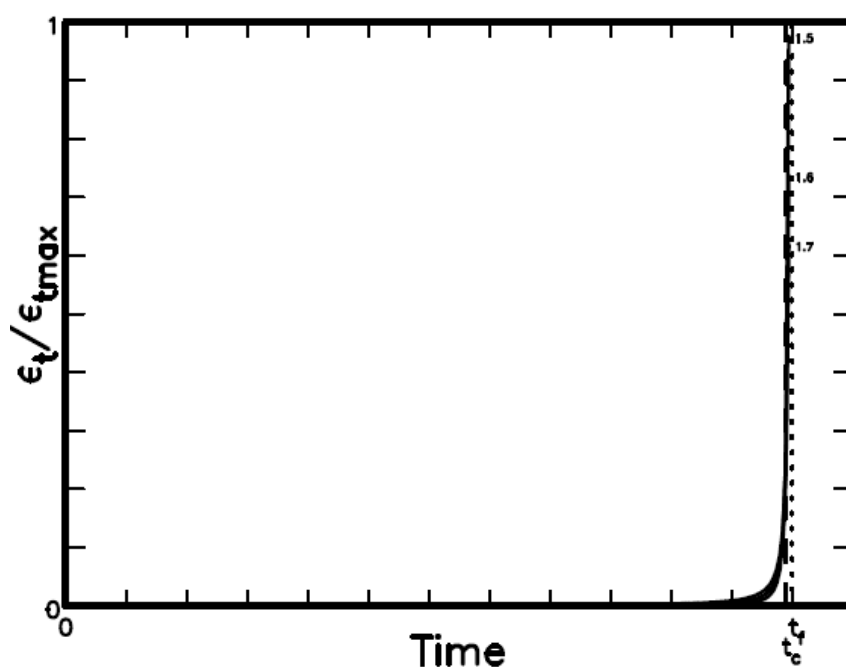


Figure 1. The plot shows the time variations in strain rate,  $\epsilon_t(t)$ , for  $\alpha=1.5$ ,  $1.6$ , and  $1.7$  when  $a=0.5$ . The three curves intersect one another at the point with  $t=t_c$ .

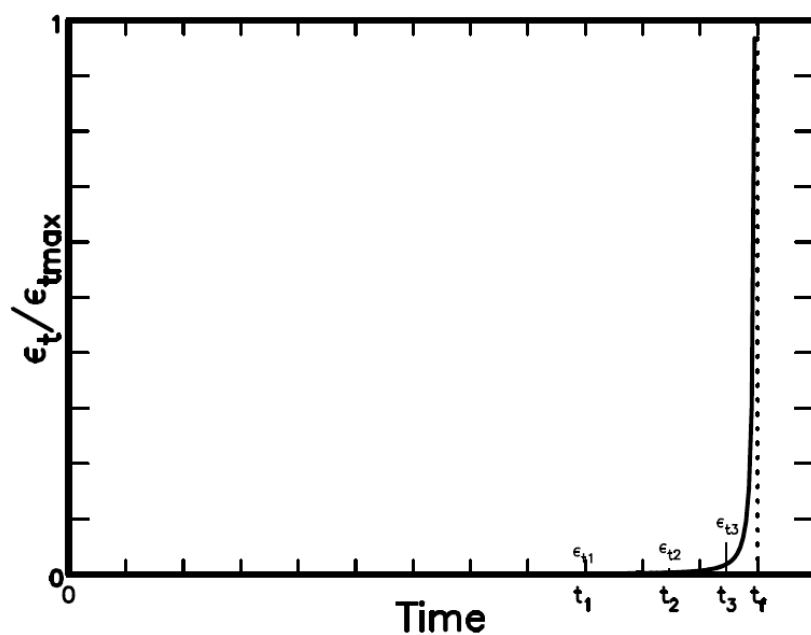


Figure 2. The plot shows the time variation in strain rate,  $\varepsilon_t(t)$ , and three values of  $\varepsilon_t(t)$ , i.e.,  $\varepsilon_{t1}$ ,  $\varepsilon_{t2}$ , and  $\varepsilon_{t3}$ , at three time instants,  $t_1$ ,  $t_2$ , and  $t_3$  for  $\alpha=1.6$  when  $a=0.5$ .

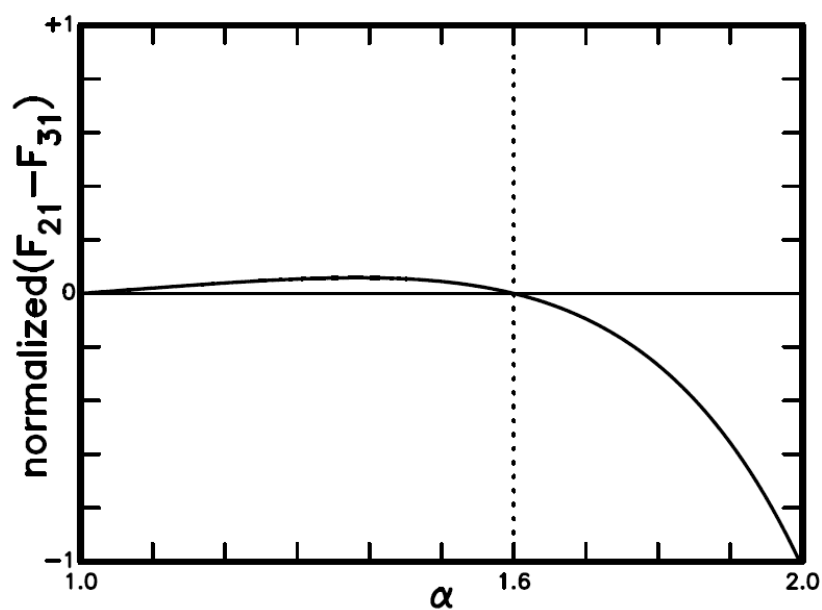


Figure 3. The plot displays the curve for  $F_{21}(\alpha)-F_{31}(\alpha)$ . The intersection point of the curve and the line with  $F_{21}(\alpha)-F_{31}(\alpha)=0$  is at  $\alpha=1.6$ .



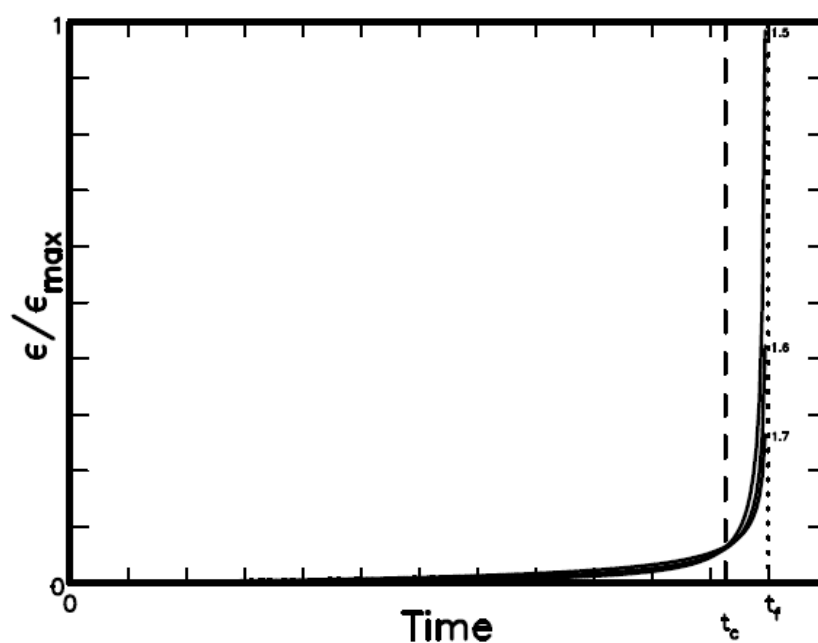
1081

1082

1083

1084

1085



1086

1087 Figure 4. The plot shows the time variations in strain,  $\varepsilon(t)$ , for  $\alpha=1.5$ , 1.6, and 1.7

1088 when  $a=0.5$ . The three curves intersect one another at the point with  $t=t_c$ .